Surface & Coatings Technology 204 (2009) 1112–1115

Contents lists available at ScienceDirect

Surface & Coatings Technology

journal homepage: www.elsevier.com/locate/surfcoat

Improvement of the performance of ZnO TFTs by low-temperature supercritical fluid technology treatment

Min-Chen Chen [a], Ting-Chang Chang [a,b,*], Sheng-Yao Huang [a], Kuan-Chang Chang [c], Hui-Chun Huang [d], Shih-Ching Chen [a], Jin Lu [a], Der-Shin Gan [d], New-Jin Ho [d], Tai-Fa Young [c], Geng-Wei Jhang [e], Ya-Hsiang Tai [e]

[a] *Department of Physics, National Sun Yat-Sen University, Kaohsiung, 804, Taiwan, ROC*
[b] *Center for Nanoscience and Nanotechnology, National Sun Yat-Sen University, Kaohsiung, 804, Taiwan, ROC*
[c] *Department of Mechanical and Electro-Mechanical Engineering, National Sun Yat-Sen University, Kaohsiung, 804, Taiwan, ROC*
[d] *Department of Materials Science and Engineering, National Sun Yat-Sen University, Kaohsiung, 804, Taiwan, ROC*
[e] *Department of Display Institute, National Chiao Tung University, Hsin-Chu, 300, Taiwan, ROC*

ARTICLE INFO

Available online 26 September 2009

Keywords:
ZnO
Supercritical fluid

ABSTRACT

In this paper, the supercritical CO_2 ($SCCO_2$) fluid technology is successfully applied to improve the electrical characteristics of sputtered ZnO TFTs at low temperature (150 °C). After the treatment of $SCCO_2$ fluids mixed with water, the ZnO TFT exhibited superior transfer characteristics and lower threshold voltage. According to X-ray photoelectron spectroscopy (XPS) analyses, the improvements were attributed to the increase of binding energies of Zn–O bonds, hydrogen-related donors and the reduction of traps at the grain boundaries in ZnO thin films. In addition, the crystalline quality and microstructure of ZnO thin films were also investigated by using X-ray diffraction (XRD) and transmission electron microscopy (TEM). The transmittance of the ZnO film was measured by an N&K analyzer 1280 (N&K Technology, Inc.), which is a new type of thin-film measurement system.

© 2009 Elsevier B.V. All rights reserved.

1. Introduction

Thin film transistors (TFTs) that are based on transparent oxide semiconductors (TOSs) have attracted much attention in the field of large area electronics due to their excellent uniformity, high transmittance in the visible light regime, and potentially better device performance and stability than conventional amorphous-Si TFT. Among several TOSs materials, TFTs that apply zinc oxide (ZnO) as the active channel layer have been extensively studied. Various growth methods, including pulsed laser deposition [1,2], chemical vapor deposition [3,4], spin-coating [5], and magnetron sputtering [6,7] have been developed to prepare the ZnO films. Magnetron sputtering is a favorable method for forming ZnO films, offering the advantage of low temperature growth, high deposition rate, and large area deposition. However, ZnO thin films deposited at low temperature without doping probably contain numerous traps and are insulating [8,9]. Therefore, high-temperature post-deposition-annealing [10] or a high deposition temperature [8] is required to decrease the number of growth defects of ZnO films. However, such a high-temperature process cannot be used for glass with a low glass transition temperature (T_g) or general plastic substrates. In this work, the supercritical CO_2 ($SCCO_2$) fluid technology, a low-temperature method, is proposed to improve the performance of sputtered ZnO TFTs at 150 °C, avoiding the above-mentioned issues that are associated with a high-temperature deposition process. The supercritical fluid exhibits liquid-like properties enabling it to carry H_2O molecules; it also exhibits gas-like properties, allowing it to diffuse into nanoscale structures without damage [11,12]. Hence, the $SCCO_2$ fluid can carry the H_2O molecules effectively into the ZnO films and passivate the traps of the deposited film at low temperature. The effectiveness of an $SCCO_2$ treatment is also discussed with respect to material analyses and electrical characteristics of the (undoped) sputtered ZnO films.

2. Experimental

The bottom-gate and bottom-contact type TFTs with the active channel layer of an undoped ZnO thin film were fabricated by applying various thin film deposition and patterning processes. The schematic cross-section view of the undoped ZnO TFTs is shown in Fig. 1. The channel width (W) and length (L) of the TFTs were 50 μm and 8 μm, respectively. As the first step of device fabrication, a 300 nm thick MoW layer was deposited by dc magnetron sputtering at room temperature on a glass substrate as a gate electrode; this layer was patterned by using conventional photolithography. Then, a 300 nm thick silicon nitride (SiN_x) layer was deposited by PECVD (Plasma Enhanced Chemical Vapor Deposition) at 350 °C as the gate insulator. A 100-nm-thick ITO film was deposited by rf (13.56 MHz) magnetron sputtering at room

* Corresponding author. Department of Physics, National Sun Yat-Sen University, Kaohsiung, 70 Lien-Hai Road, Kaohsiung, Taiwan, ROC. Tel.: +886 7 5252000 3708; fax: +886 7 5253709.
E-mail address: tcchang@mail.phys.nsysu.edu.tw (T.-C. Chang).

0257-8972/$ – see front matter © 2009 Elsevier B.V. All rights reserved.
doi:10.1016/j.surfcoat.2009.09.050

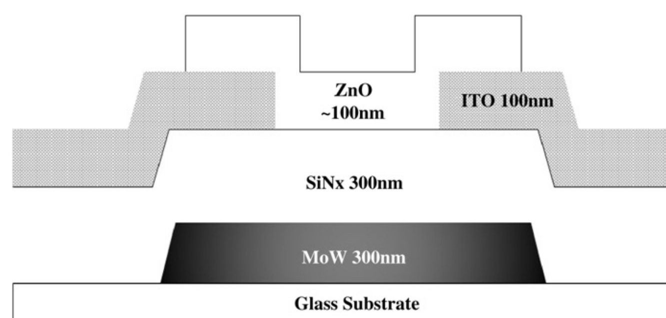

Fig. 1. Schematic cross-section view of the fabricated ZnO TFT structure.

temperature and patterned using photolithography to form the source/drain electrodes. Finally, a 100-nm-thick undoped ZnO film was deposited at room temperature by rf magnetron sputtering of a ZnO target (101.6 mm in diameter, 99.999%). The ZnO target was sputtered with an rf power of 100 W under pure Ar ambience. The Ar gas flow was 30 sccm and the pressure was maintained at 0.53 Pa. The active layer was defined using photolithography and wet etching. Subsequently, different post-treatment methods were performed on the undoped ZnO films to improve the electric characteristics. During the treatment, marked as "H_2O vapor treatment", the sample was placed in a stainless steel chamber filled with H_2O vapor at 150 °C for 1 h. For another treatment, marked as "heat treatment", the sample was annealed under air atmosphere in the chamber at 150 °C for 1 h. The other sample, marked as "$SCCO_2$ treatment", was placed in a supercritical fluid system at 150 °C for 1 h, where it was injected with a 2.06×10^7 Pa $SCCO_2$ fluid mixed with 5 ml pure H_2O. In addition, ZnO TFTs without any treatment were taken as reference samples marked as "standard." After these different treatments, the electrical characteristics of the device were measured using an Agilent 4156C semiconductor parameter analyzer in the dark environment at room temperature. The crystalline quality and crystal orientation of ZnO thin films deposited on Si wafer were investigated by X-ray diffraction (XRD). In addition, the microstructure and chemical bonding states of these treated-ZnO films were analyzed with transmission electron microscopy (TEM) and X-ray photoelectron spectroscopy (XPS).

3. Results and discussion

Fig. 2 plots the transfer characteristics of the TFTs that have undergone room temperature deposition and subsequent post-treatment under different conditions. The threshold voltage (V_T) was defined as the gate voltage at which the drain current reaches 10^{-10}A. A standard TFT does

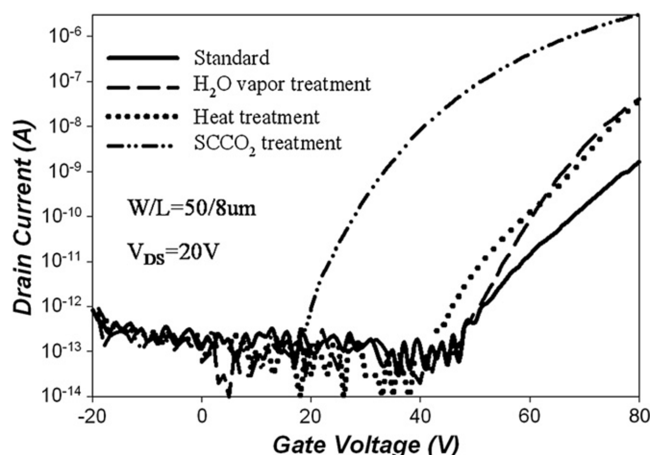

Fig. 2. Transfer characteristics of undoped ZnO TFTs in as-deposited state and after post-treatments.

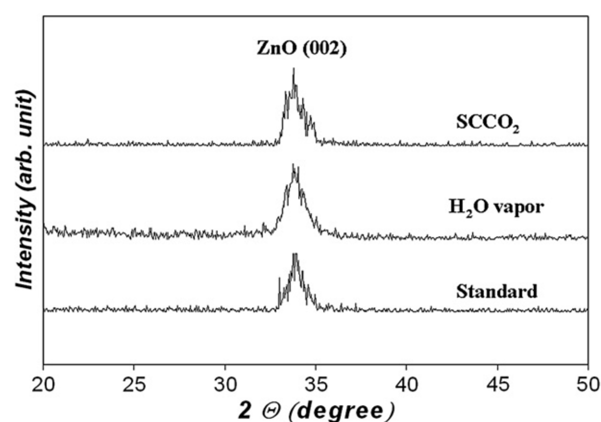

Fig. 3. X-ray diffraction spectra of ZnO films before and after post-treatments.

not have acceptable transistor characteristics with a threshold voltage of 65.81 V, the subthreshold swing of 8.29 V/decade, and the mobility of 2.82×10^{-5}. The drain current, subthreshold swing and mobility of the ZnO device treated with H_2O vapor slightly improved to 4.9×10^{-8}A, 4.93 V/decade, and 1.01×10^{-3}, respectively. However, the threshold voltage (60.01 V) remained large. Additionally, the electrical properties of the heat treatment TFTs show a similar behavior to the H_2O vapor treatment TFTs. It is also indicated that the temperature at 150 °C was not high enough to improve the film quality. Clearly, the $SCCO_2$ treatment TFTs have a significantly improved performance compared to the above devices, as shown by threshold voltage of 27.92 V, subthreshold swing of 3.93 V/decade, mobility of 2.6×10^{-2}, and on/off current ratio of approximately 10^6. The experimental results show that the $SCCO_2$ fluid is appropriate to improve the properties of the device due to its high diffusion ability.

The electrical properties of the film are determined by its structure, especially the growth defects and crystal imperfections. Fig. 3 presents the XRD spectra of the ZnO films before and after post-treatment. As can be seen, all samples exhibit a similar peak at about 34°, corresponding to the (002) plane with the crystallized phase of the wurtzite structure, indicating a preferred orientation with the *c*-axis perpendicular to the surface of the substrate [13]. Fig. 4 shows the cross-sectional TEM images of the ZnO films under various treatment conditions (a) standard, (b) treated with H_2O vapor and (c) treated with $SCCO_2$ fluid. The thicknesses are 107 nm, 110 nm, and 100 nm, respectively. The inset in Fig. 4(a)–(c) displays electron diffraction patterns taken from a region of a ZnO thin film. The ring pattern indicates that the ZnO films are polycrystalline wurtzite structures, containing many crystalline grains [14]. Even after post-treatment, the grain size, crystallized phase and orientation are approximately the same as those of the standard sample. Therefore, the improvement in device characteristics is not associated with the film structure, but perhaps with passivation of the dangling bonds (or traps).

Since there are many ZnO grains in the as-deposited ZnO film, the traps at the grain boundaries may establish a potential barrier when the device is operated, producing a low drain current and a high threshold voltage. Although H_2O vapor treatment increases the current, a large threshold voltage still existed, suggesting that only some of the traps were passivated. Therefore, most of the traps at the grain boundaries were passivated by $SCCO_2$ treatment, substantially improving the characteristics of the device.

XPS measurements were made to determine the qualitative and quantitative composition of the ZnO films after post-treatments, and the binding energies were calibrated by taking the carbon C 1s peak (285.0 eV) as a reference. Fig. 5 shows the (a) Zn 2p3/2 and (b) O 1s of the XPS spectra of ZnO films after various treatments. The Zn 2p3/2 peak of the standard sample centered at about 1021.6 eV corresponds to Zn–O bonds [15]. After post-treatment, the peaks shifted to higher binding

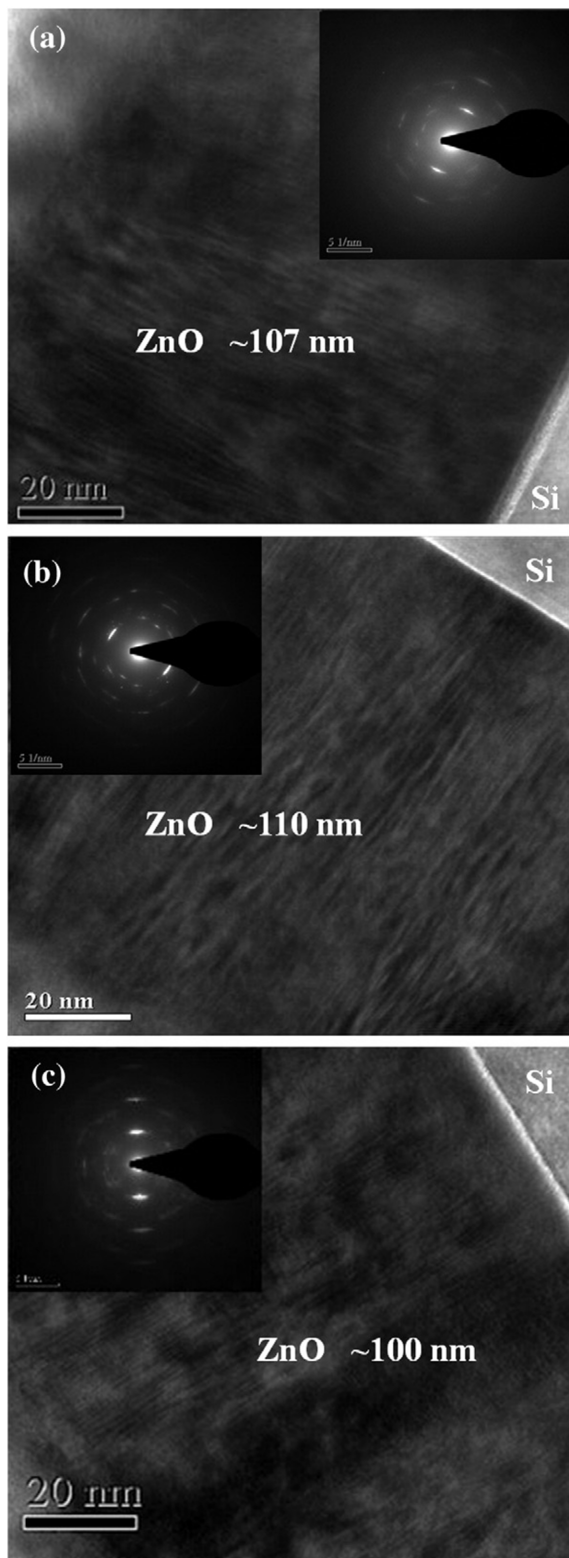

Fig. 4. Cross-sectional TEM images and diffraction patterns (inset) of the ZnO thin films after various treatment conditions, including (a) standard, (b) H_2O vapor, (c) $SCCO_2$.

energies, at 1021.9 and 1022.1 eV, respectively. The increases of binding energy indicated that Zn atoms in ZnO film have been oxidized more completely with surrounding oxygen atoms. It also confirms that the H_2O molecules excellently oxidize Zn atoms, and that the $SCCO_2$ fluid is more efficient than H_2O vapor in transporting H_2O molecules into the ZnO film. As shown in Fig. 5(b), the O 1s peak can be fitted by two nearly Gaussian distributions, centered at 530.0 eV and 531.6 eV corresponding to O–Zn and O–H bonds, respectively. The O–H bonding is caused by the adsorption of H_2O molecules on the ZnO film [16]. However, the standard sample without any post-treatment also contains O–H bonds, because ZnO films are exposed to air, causing the H_2O to be adsorbed on the surface. Additionally, the H_2O molecules that were absorbed in ZnO thin films dissociated into H and OH groups, which rapidly diffused into the ZnO film [17].

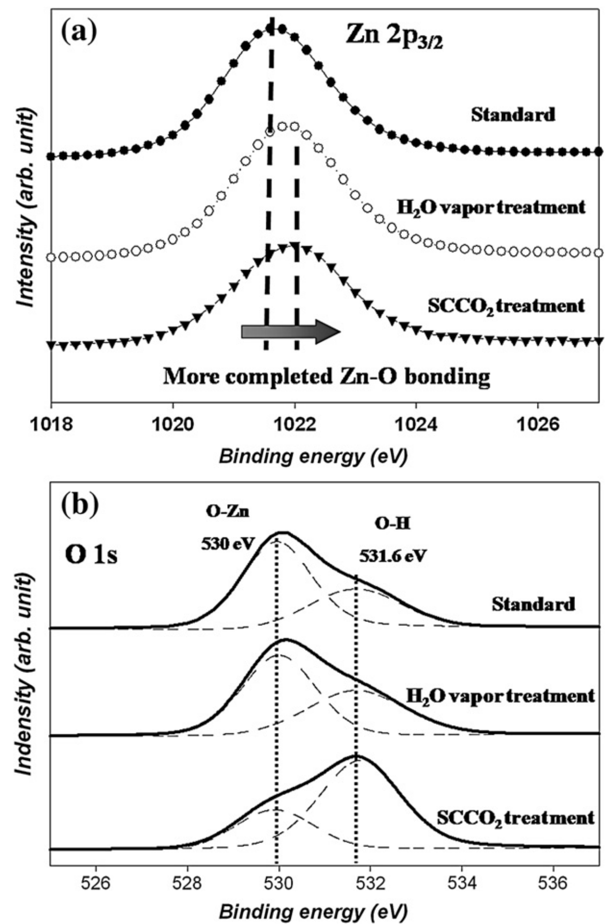

Fig. 5. The (a) Zn $2p_{3/2}$ (b) O 1s XPS spectra of ZnO thin films after various treatment conditions.

As previous studies reported, the hydrogen atoms can be incorporated into ZnO to form hydrogen-related donors, such as the substitutional hydrogen bound to zinc atoms and the interstitial hydrogen bound to oxygen atoms, and improve the electrical conductivity of ZnO films [18–21]. On the other hand, Zn–OH bonds can also be formed by the passivation of the dangling bonds (or traps) in the grain boundaries by OH. Therefore, the potential barrier that is induced by the dangling bonds can be suppressed.

To compare the ratios of the components of O–Zn and O–H, the individual peak areas were integrated with the effect of sensitivity factors, as shown in Table 1. The percentages of O–H bonding for the standard sample, the ZnO film after treatment with H_2O vapor and

Table 1
Ratios of O–Zn and O–H calculated from XPS O 1s signal of the ZnO films after various treatment conditions.

	O–Zn/O (%)	O–H/O (%)
Standard	66.38	33.62
H_2O vapor	58.08	41.92
$SCCO_2$	38.13	61.87

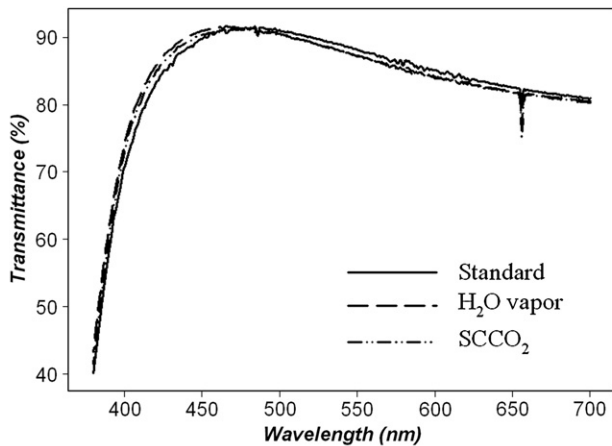

Fig. 6. Transmittance of ZnO films on a glass substrate under various treatments.

$SCCO_2$ treatment are 15.02%, 16.36% and 46.13%, respectively. These results demonstrate that H_2O molecules were effectively carried into the ZnO film by the highly-diffusing $SCCO_2$ fluid, passivating the traps. In future work, secondary ion mass spectroscopy (SIMS) will be performed to analyze the hydrogen distribution in the ZnO films as a further evidence for our proposed model.

To investigate the effect of various treatments on the transmittance of ZnO films and prevent the influence of Si substrates, the ZnO films were deposited on glass substrates under the same deposition conditions. Fig. 6 shows the transmittance spectra of the ZnO films after post-treatments. Clearly, the transmittance values for all samples are almost the same: the high transmittance exceeds 80% in the wavelength range from 430 nm to 700 nm.

To test the electrical stability of the ZnO TFTs after $SCCO_2$ treatment, a prolonged gate bias stress was applied to investigate the degradation of the current. The device was stressed at $V_{GS} = 20\text{ V} + V_T$ for 1000 s while the source and drain were grounded. Fig. 7 shows the shifts of the transfer characteristic after the gate bias stress and the recovery characteristic (measured after standing for 1000 s). Evidently, the threshold voltage after stress is shifted in the positive direction, but the shape of the transfer curve is nearly unchanged compared to the initial curve. Since the subthreshold swing is not varied, the degradation is attributed mainly to charge trapping in the bulk dielectric layers or at the channel/dielectric interface [22,23]. Furthermore, the stressed transfer characteristic recovered rapidly within 1000 s to the initial characteristic due to charge de-trapping. Thus, the degradation is caused by transient charge trapping.

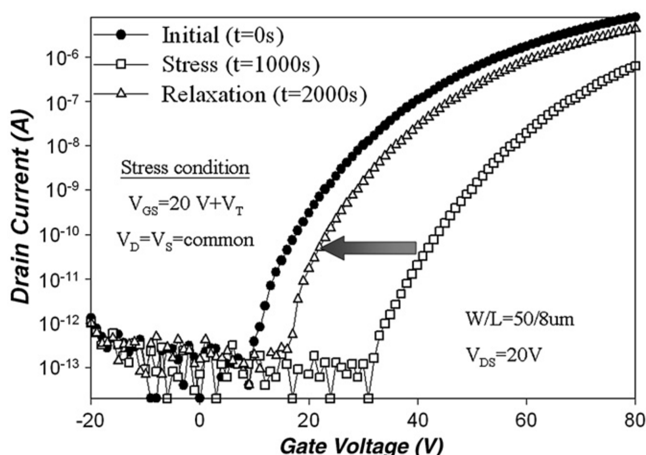

Fig. 7. Comparison of the transfer curves of the ZnO TFTs after $SCCO_2$ treatment measure before bias stress ($t = 0$ s), after bias stress ($t = 1000$ s) and after relaxation ($t = 2000$ s).

4. Conclusions

The effects of low-temperature $SCCO_2$ treatments on the ZnO films have been demonstrated experimentally. The preliminary improvement is obtained by H_2O vapor treatment attributed to the H_2O absorbed in ZnO thin films, and the hydrogen atoms can be incorporated into ZnO to form hydrogen-related donors. Besides, the dangling bonds (or traps) in the grain boundaries can be passivated by OH and form Zn–OH bonds. A further investigation verifies that traps passivation efficiency can be optimized by the $SCCO_2$ treatment, because the $SCCO_2$ fluid could more effectively transport H_2O molecules into ZnO films. Therefore, a lower potential barrier at grain boundaries results in the significantly improved device characteristics. From XRD and TEM, the grain size and crystal orientation are approximately unchanged which means $SCCO_2$ fluids can diffuse into the nanoscale structures without damage. Moreover, the treated ZnO films still exhibit high transmittance above 80% within the visible light range. The changes of threshold voltage under gate bias stress do not require any thermal/bias annealing for the devices to recover their initial state, which is caused by the effect of a transient charge trapping in the bulk dielectric or at the channel/dielectric interface.

Acknowledgments

This work was performed at National Science Council Core Facilities Laboratory for Nano-Science and Nano-Technology in Kaohsiung–Pingtung area and was supported by the National Science Council of the Republic of China under Contract Nos. NSC-97-3114-M-110-001 and NSC 97-2112-M-110-009-MY3.

References

[1] S. Masuda, K. Kitamura, Y. Okumura, S. Miyatake, H. Tabata, T. Kawai, J. Appl. Phys. 93 (2003) 1624.
[2] V. Craciun, J. Elders, J.G.E. Gardenievs, I.W. Boyd, Appl. Phys. Lett. 65 (1994) 2963.
[3] K. Minegishi, Y. Koiwai, Y. Kikuchi, K. Yano, M. Kasuga, A. Shimizu, Jpn. J. Appl. Phys., Part 2 36 (1997) 1453.
[4] M. Purica, E. Budianu, E. Rusu, M. Danila, R. Gavrila, Thin Solid Films 403–404 (2002) 485.
[5] B.J. Norris, J. Anderson, J.F. Wager, D.A. Keszler, J. Phys. D 36 (2003) L105.
[6] G. Xiong, J. Wilkinson, B. Mischuck, S. Tuzemen, K.B. Ucer, R.T. Williams, Appl. Phys. Lett. 80 (2002) 1195.
[7] K.B. Sundaram, A. Khan, Thin Solid Films 295 (1997) 87.
[8] H.S. Bae, J.H. Kim, S. Im, Electrochem. Solid-State Lett. 7 (2004) G279.
[9] J.Y. Lee, Y.S. Choi, W.H. Choi, H.W. Yeom, Y.K. Yoon, J.H. Kim, S. Im, Thin Solid Films 420–421 (2002) 112.
[10] H.Q. Chiang, J.F. Wager, R.L. Hoffman, J. Jeong, D.A. Keszler, Appl. Phys. Lett. 86 (2005) 13503.
[11] C.T. Tsai, P.T. Liu, T.C. Chang, C.W. Wang, P.Y. Yang, F.S. Yeh, IEEE Trans. Electron Device Lett. 28 (7) (2007) 584.
[12] C.T. Tsai, T.C. Chang, P.T. Liu, P.Y. Yang, Y.C. Kuo, K.T. Kin, P.L. Chang, F.S. Yeh, Appl. Phys. Lett. 91 (2007) 012109.
[13] L.W. Lai, C.T. Lee, Mater. Chem. Phys. 110 (2008) 393.
[14] S.J. Henley, M.N.R. Ashfold, D. Cherns, Surf. Coat. Tech. 177 (2004) 271.
[15] C.X. Xu, X.W. Sun, X.H. Zhang, L. Ke, S.J. Chua, Nanotechnology 15 (2004) 856.
[16] L.J. Meng, C.P. Moreira, M.P. d. Santos, Appl. Surf. Sci. 78 (1994) 57.
[17] Y.F. Lu, H.Q. Ni, Z.H. Mai, Z.M. Ren, J. Appl. Phys. 88 (2000) 498.
[18] M.S. Oh, D.K. Hwang, J.H. Lim, Y.S. Choi, S.J. Park, Appl. Phys. Lett. 91 (2007) 212102.
[19] C.G. Van de Walle, Phys. Rev. Lett. 85 (2000) 1012.
[20] C. Kilic, A. Zunger, Appl. Phys. Lett. 81 (2002) 73.
[21] J.B.L. Martins, C.A. Taft, S.K. Lie, E. Longo, J. Mol. Struct. (Theochem) 528 (2000) 161.
[22] A. Suresh, P. Wellenius, J.F. Muth, Tech. Dig. – Int. Electron Devices Meet. (2007) 587.
[23] M.J. Power, C.V. Berkel, A.R. Franklin, S.C. Deane, W.I. Milne, Phys. Rev. B 45 (1992) 4160.